Appl Microbiol Biotechnol (2017) 101:7201–7212
DOI 10.1007/s00253-017-8454-7

Recombinant expression and biochemical characterization of *Mycobacterium tuberculosis* 3Fe-4S ferredoxin Rv1786

Yun Lu[1] · Feng Qiao[1] · Yue Li[1] · Xiao-Hong Sang[1] · Cong-Ran Li[1] · Jian-Dong Jiang[1] · Xin-Yi Yang[1] · Xue-Fu You[1]

Received: 23 May 2017 / Revised: 24 July 2017 / Accepted: 26 July 2017 / Published online: 15 August 2017

Abstract Ferredoxins are iron-sulfur protein that mediate electron transfer in cytochrome P450 mono-oxygenase (CYP)-related catalytic reactions in a wide variety of organisms. Rv1786 is a putative ferredoxin, encoded by a gene located downstream of the gene encoding CYP143A1 in the *Mycobacterium tuberculosis* genome. However, the structure and function of Rv1786 have remained unclear. Here, the recombinant *Mtb* Rv1786 was expressed, purified as a His-tagged form and characterized with [3Fe-4S] clusters as its cofactors using a series of measurements including SDS-PAGE, western blot, UV/Visible, MALDI-TOF/TOF-MS, and electron paramagnetic resonance spectroscopic analysis. Based on the assessments of surface plasmon resonance (SPR) and steady state kinetic assays, Rv1786 was found to be able to couple with both ferredoxin reductase A (FdrA) and flavoprotein reductase A (FprA) as redox partner, but with a stronger binding to FprA and a better coupling activity to FdrA. Preliminary structural and biochemical characterization of *Mtb* Rv1786 as a redox partner is presented here.

Xin-Yi Yang and Xue-Fu You contributed equally to this work

Electronic supplementary material The online version of this article (doi:10.1007/s00253-017-8454-7) contains supplementary material, which is available to authorized users.

✉ Xin-Yi Yang
yangxinyi1976@hotmail.com

✉ Xue-Fu You
xuefuyou@hotmail.com

[1] Laboratory of Pharmacology/Beijing Key Laboratory of Antimicrobial Agents, Institute of Medicinal Biotechnology, Chinese Academy of Medical Sciences and Peking Union Medical College, Beijing 100050, China

Keywords *M. tuberculosis* · Ferredoxin · Rv1786 · Cytochrome P450 mono-oxygenase redox partner · Ferredoxin reductase A · Flavoprotein reductase A

Introduction

Tuberculosis (TB) caused by *Mycobacterium tuberculosis* (*Mtb*) remains one of the leading causes of death worldwide. According to statistical data from the World Health Organization (WHO), about 10.4 million people became ill with TB and 1.4 million died from the disease in 2015 (WHO 2016). Over the past 40 years, an effective four-drug combination regimen of isoniazid, rifampicin, pyrazinamide, and ethambutol has been developed and employed as the first choice for TB treatment. However, long-term use of a limited number of drugs has led to significant non-compliance, side effects, and drug resistance (Riccardi et al. 2009). The prevalence of multidrug-resistant (MDR) and extensively drug resistant (XDR) *Mtb* strains has become a new serious public health problem in many countries (Lauzardo and Peloquin 2012). Thus, there is an urgent need to find new anti-TB drugs with novel targets.

Ferredoxins are acidic, low molecular weight, soluble iron-sulfur proteins that exist in diverse organisms. Ferredoxins mainly act as electron transfers in redox systems that are involved in a range of important metabolic processes such as cytochrome P450-associated reactions (i.e., hydroxylation, epoxidation, peroxidation, sulfoxidation, dealkylation, or deamination of a substrate) (Ewen et al. 2011). In bacteria, a classic cytochrome P450 mono-oxygenase (CYP) system generally consists of a ferredoxin, a ferredoxin-NAD(P)H reductase (FNR), and the CYP. Electrons required for a CYP catalytic reaction are transferred from a reduced nicotinamide cofactor, such as NADH or NADPH, to the CYP via FNR and

ferredoxin (Werck-Reichhart and Feyereisen 2000). The general electron transfer pathway for a bacterial CYP system follows as NAD(P)H → FNR → ferredoxin → CYP (Ewen et al. 2011). The genome sequence of *Mtb* revealed that the pathogen encodes 20 different CYPs with five ferredoxins, two FNRs (FdrA and FprA), and two FDRX (fusion protein of FNR and ferredoxin) as their putative electron transfer partners (Munro et al. 2003).

In recent studies, some of the *Mtb* CYPs and their redox partners were found to be essential for the pathogen's viability or pathogenicity and have been suggested to be potential candidates for *Mtb* drug targeting (Fischer et al. 2002; Ouellet et al. 2010; Zhang et al. 2006). However, identification of the correct redox partners for CYPs in *Mtb* remains a big challenge since only a minority of CYPs and CYP-related redox proteins have been structurally and/or functionally characterized, and as redox protein-coding genes normally are distant from most of the CYP genes at their genomic loci. In addition, heterologous expression of *Mtb* CYPs or putative redox partner proteins in other host system, such as in *Escherichia coli*, has often remained unsuccessful and ineffective. This has further impeded characterization of the redox system for the pathogen (McLean et al. 2006a, b). Among the five putative ferredoxins, including FdX (*Rv0763c*), Rv1786 (*Rv1786*), FdxA (*Rv2007c*), FdxC (*Rv1177*), and FdxD (*Rv3503c*), in *Mtb* pathogenic strain H37Rv, to date, only FdX has been identified as a redox partner to support catalysis with CYP51, while all the rest ferredoxins have remained poorly characterized for their structures or functions (Ouellet et al. 2010).

Rv1786, a putative 3Fe-4S ferredoxin encoded by H37Rv gene *Rv1786*, is located downstream of CYP143A1 (*Rv1785c*) and has been considered a potential natural electron transfer partner protein for CYP143A1. Despite the fact that little is currently known about the structure or possible functions of CYP143A1, it appears to be highly conserved across the *Mycobacterium* genus including pathogenic and non-pathogenic species by phylogenetic analysis, which suggests the CYP enzyme may perform important general functions in *Mtb*. Hence, given the adjacent location of Rv1786 to CYP143A1, characterizing the structural and biochemical properties of Rv1786 and validating the members of the Rv1786-based redox couples would be very useful for further understanding of the potential catalytic activity of the CYP enzyme.

In this study, *Rv1786* from the highly pathogenic *Mtb* strain H37Rv was heterologously expressed in *E. coli*, purified as a His-tagged construct and characterized by SDS-PAGE, western blot, MALDI-TOF/TOF-MS, UV/Visible (UV/Vis), and electron paramagnetic resonance (EPR) spectroscopic analysis. To reveal possible reductase partners of Rv1786 in redox coupling system, interactions between Rv1786 and each of FdrA, FprA, and CYP143A1 were evaluated by surface plasmon resonance (SPR) assays and steady state kinetic studies. Our results show that although both reductase proteins appeared to be involved in transferring electron from Rv1786, FprA had a stronger binding affinity for Rv1786, and FdrA had a better coupling activity with Rv1786. To the best of our knowledge, this is the first report on the preliminary structural and biochemical characterization of *Mtb* Rv1786 as a redox partner.

Materials and methods

Template DNA, strains, and plasmid

Genomic DNA from *Mtb* strain H37Rv, which was kindly provided by Dr. J. Xu and Y. Lu, Department of Pharmacology, Beijing Tuberculosis and Thoracic Tumor Research Institute, Beijing Chest Hospital, was used as template DNA in this study. The *Mtb* strain H37Rv was deposited at the American Type Culture Collection as ATCC 25618. *E. coli* strains DH5α, BL21 (DE3), and Rosetta (DE3) as well as plasmid pET30a were used for cloning and expression. The *E. coli* strains DH5α and BL21 (DE3) were obtained from TaKaRa (Dalian, China), and the *E. coli* strain Rosetta (DE3) was obtained from TransGen Biotech (Beijing, China). The plasmid pET30a was purchased from Novagen (Madison, WI, USA). *E. coli* strains transformed with plasmids were cultured in LB (Luria-Bertani) medium (Oxoid, Basingstoke, UK) supplemented with appropriate antibiotics. Oligonucleotide primers for gene amplification, and containing appropriate restriction sites for cloning (Table 1), were synthesized by Shanghai Invitrogen (Shanghai, China).

DNA manipulations

General DNA manipulations were carried out following standard protocols as described by Sambrook et al. (Sambrook and Russell 2006). Plasmid DNA was isolated with the EasyPure HiPure Plasmid MiniPrep Kit (TransGen Biotech, Beijing, China). PCR amplification products were purified from agarose gels with the EasyPure Quick Gel Extraction Kit (TransGen Biotech, Beijing, China).

Sequence alignment and phylogenetic analysis

All ferredoxin protein sequences were obtained from NCBI database. Since Rv1786 belongs to the putative ferredoxin with [3Fe-4S] cluster, all protein sequence alignments of ferredoxins with [3Fe-4S] cluster were analyzed. The resulting output sequences for various species were aligned and saved in ClustalX 2.0 format (Takagi et al. 2005). A phylogenetic tree was generated using MEGA 5.0 software (Oluwatoyin Japhet et al. 2012). The aligned ClustalX 2.0 format sequences

Table 1 Oligonucleotide primers used in plasmid construction

Primer	Sequence
Rv1786 F	5′-AG**CATATG**AAAGTCCGTCTCGATCCA-3′
Rv1786 R	5′-AT**AAGCTT**CAGTGATGGTGATGGTCCGCGTCGTCCTCCTCGAGGAT-3′
FdrA F	5′-C**CATATG**AACGCACACGTGACCAGTCGTGAA-3′
FdrA R	5′-TGT**CTCGAG**GGCCTGAGTTTGGTCTAACACT-3′
FprA F	5′-CA**CATATG**CGTCCCTATTACATCGCCATCG-3′
FprA R	5′-A**CTCGAG**GCCGAGCCCAATCCGCAACAG-3′
CYP143A1 F	5′-GAC**CATATG**ACCACCCCCGGCGAGGACCACGC-3′
CYP143A1 R	5′-GAA**AAGCTT**CAGTGATGGTGATGGCTCCAGCGTAG-CGGCAAGTTCTTA-3′

were imported into the MEGA phylogeny tool, and a phylogenetic tree was generated using the "construct/test maximum likelihood" method.

Cloning of the genes coding for Rv1786, FdrA, FprA, and CYP143A1

Mtb gene *Rv1786* (GeneID 885846) was amplified from the genomic DNA of *Mtb* strain H37Rv (NC_000962.2) by PCR using PrimeSTAR® HS DNA Polymerase with GC buffer (TaKaRa, Dalian, China). Primers used for amplification of *Rv1786* gene are listed in Table 1. The forward primer contained a *Nde*I restriction site permitting cloning into the start codon (ATG) of pET30a, while the reverse primer was designed to produce an in-frame tetrahistidine C-terminal tag (underlined) and a stop codon (TGA) followed with a *Hind* III restriction site. The amplification conditions were 98 °C for 3 min; then 30 cycles of 98 °C for 15 s, 56 °C for 15 s, and 72 °C for 20 s; and finally, 72 °C for 10 min. The amplicon was ligated into a similarly restricted pET30a vector and introduced by transformation into *E. coli* Rosetta (DE3) (TransGen Biotech, Beijing, China), and resulting kanamycin- and chloramphenicol-resistant colonies containing the cloned *Rv1786* were confirmed by PCR and sequencing. One of these clones, pET30a-*Rv1786*, was chosen for further study.

Mtb genes for FdrA (*Rv0688*), FprA (*Rv3106*), and CYP143A1(*Rv1785c*) were also amplified from the genomic DNA of *Mtb* H37Rv with primers in Table 1 by PCR using PrimeSTAR® HS DNA Polymerase with GC buffer (TaKaRa, Dalian, China). The amplification conditions of FdrA and FprA were 98 °C for 3 min; then 30 cycles of 98 °C for 15 s, 56 °C for 15 s, and 72 °C for 90 s; and finally, 72 °C for 10 min. The amplification conditions of CYP143A1 were different from the other genes, as an extra process called touchdown PCR was added before the normal process. The total conditions of CYP143A1 were 98 °C for 2 min, then 20 cycles of 98 °C for 10 s, 75 °C for 15 s, and 1 °C minus per cycle, then 68 °C for 2 min, followed by a normal PCR process. All the amplicons were ligated into corresponding restricted pET30a vector and transformed into *E. coli* BL21 (DE3) (TaKaRa, Dalian, China), and resulting kanamycin-resistant colonies containing the cloned FdrA, FprA, or CYP143A1 were confirmed by colony PCR and sequencing, respectively. Positive clones were chosen for further study.

Expression, purification, and spectra analysis of Rv1786, FdrA, FprA, and CYP143A1

Transformant *E. coli* Rosetta (DE3) cells containing pET30a-*Rv1786* were incubated in LB medium supplemented with 30 μg/mL kanamycin and 34 μg/mL chloramphenicol at 37 °C until the OD_{600} reading was up to 0.6. Then, 0.5 mM isopropyl 1-thio-β-D-galactopyranoside (IPTG) was added to induce target gene expression. The transformant cells were then incubated for a further 4 h. The cells were harvested by centrifugation at 6000×*g* for 10 min at 4 °C, washed with 0.85% NaCl twice, and resuspended in PBS (pH 7.4). The cells were lysed on ice by ultrasonication for 20 min with cycles of 2-s sonication followed by 6-s rest. After centrifugation at 12,000×*g*, 4 °C for 20 min, the supernatants were loaded onto Ni-IDA-Sefinose™ Resin (Sangon Biotech, Shanghai, China). The brown-colored fractions were eluted with a linear gradient of 20–500 mM imidazole. Each eluted fraction was analyzed by SDS-PAGE. Fractions containing relatively pure protein were pooled and concentrated to a volume of approximately 2 mL using ultrafiltration with Amicon concentrators (Merck Millipore, MA, USA) at 4 °C. After dialysis against 50 mM Tris-HCl (pH 7.4) overnight to remove excess imidazole, the fractions were loaded onto Q Sefinose™ FF agarose (Sangon Biotech, Shanghai, China) and eluted with a gradient NaCl/Tris-HCl buffer (pH 6.0). Samples were pooled and concentrated to 100 μL by ultrafiltration using Amicon concentrators at 1500×*g*. The concentrated samples were further dialyzed into 50 mM Tris-HCl (pH 7.4). A final purification step was performed for the concentrated protein via a Superdex 75 10/300GL using an AKTA purification system (GE Healthcare, Pittsburgh, PA). Eluted fractions were again analyzed by SDS-PAGE. The fractions were pooled and concentrated as before, and dialyzed into 50 mM Tris-HCl, pH 7.4, and stored at −80 °C until use.

Procedures used for the expression and purification of FdrA, FprA, and CYP143A1 were the same as described for Rv1786 above, except that the induction of the expression for FdrA and FprA was carried out with 1 mM IPTG at 22 and 25 °C, respectively. The expression of CYP143A1 (*Rv1785c*) was induced with 0.75 mM IPTG at 22 °C in the presence of the heme precursor delta-aminolevulinic acid (ΔALA; 100 μM).

SDS-PAGE and UV/Vis spectrophotometry analyses were performed to identify the purity, correct molecular weight, and recognizable absorption spectrum of the purified proteins containing iron-sulfur cluster. The UV/Vis spectroscopic analysis of the samples was carried out in 96-well plate (Corning, MA, USA). All the proteins were examined by PerkinElmer EnSpire® 2300 Multimode Plate Readerz (PerkinElmer, MA, USA) in potassium phosphate buffer (pH 7.4). The wavelength range used for spectral scanning was 260 to 700 nm.

Western blot analysis and EPR spectroscopic analysis of Rv1786

Western blot analysis was performed to confirm the correct expression of His_4-tagged purified Rv1786 protein. One microgram of purified protein was loaded in 12% gel and separated by SDS-PAGE. The sponge and filter paper were presoaked in transfer buffer (25 mM Tris base, 190 mM glycine, 20% methanol). A polyvinylidene fluoride (PVDF; pore size 0.22 μm; Millipore, MA, USA) membrane was cut to the same size of the gel and submerged into 10 mL of 100% methanol for 5 min. The protein was transferred onto the PVDF membrane in transfer buffer at 250 mA for 90 min at room temperature (RT). The blotted PVDF membrane was incubated in 5% skim milk in Tris-buffered saline (TBS) with Tween-20 (TBST) at RT for 1 h with shaking to block nonspecific binding. The membrane was then incubated overnight at 4 °C with rabbit polyclonal anti-His_4 tag antibody (Sangon Biotech, Shanghai, China) diluted 1:500 *v*/*v* with TBST containing 5% skim milk. After a washing step, the membrane was incubated with horse radish peroxidase (HPR)-conjugated goat anti-rabbit IgG antibody (Sigma, St. Louis, MO, USA) diluted 1:5000 *v*/*v* in 5% skim milk TBST. Subsequently, the membrane was stained using 3,3′,5,5′-tetramethylbenzidine (TMB; Sigma, St. Louis, MO, USA) as the electrochemical substrate of HPR.

Test samples of the purified *Mtb* Rv1786 protein for EPR spectroscopy were prepared at a concentration of 1.25 mg/mL in 50 mM Tris buffer. EPR spectra of Rv1786 protein were recorded at 10 K using a Bruker E580 spectrometer operated at X-band with a modulation frequency of 9.371 GHz and an incident microwave power of 2.377 mW. The sweep time was set as 120 s and modulation amplitude (g) was 1.000 G. Rv1786 spectra in both the oxidized and sodium dithionite-reduced forms were recorded.

MALDI-TOF/TOF-MS of Rv1786

The molecular mass of the purified *Mtb* Rv1786 protein was determined using a Bruker Ultraflex III MALDI-TOF/TOF-MS spectrometer equipped with Smart-beam laser (200 Hz). The matrix-assisted laser desorption/ionization MALDI-TOF/TOF MS result was obtained in the liner positive mode with an accelerating voltage of 20 kV. The protein samples were dissolved in Tris-HCl to a concentration of 1.25 mg/mL (pH 7.4). Theoretical molecular mass of the protein was calculated by the Compute pI/Mw tool.

SPR analysis

The protein-protein interactions between Rv1786 and each of FprA, FdrA, and CYP143A1 were analyzed by PlexArray HT (V3 version) label-free biomolecular interaction detection system (Plexera Bioscience, Seattle, WA, USA), which is based on SPR biosensing technology as described previously (Hu et al. 2014; Wu et al. 2015; Zhu et al. 2014). Rv1786 was dissolved in 25 mM Tris-HCl (pH 8.0) to achieve a concentration of 0.5 mg/mL, and immobilized onto a Nanocapture sensor chip (Plexera Bioscience, Seattle, WA, USA) by QArray mini spotter (Genetix Ltd., New Milton, Hampshire, UK) at 25 °C with humidity at 65%. Each sample was spotted in replicate on the chip, and each spot contained 0.1 μL of sample solution. During each measurement cycle, PBS running buffer (10 mM, pH 6.4) was first flowed through the chip surface at a rate of 2 μL/s to obtain a stable baseline, and the purified FprA, FdrA, or CYP143A1 was then injected as analyte at various concentrations in the running buffer for detecting their binding affinity to Rv1786 fixed on the chip surface. For binding measurements, four different concentrations of each analyte protein (500, 1000, 2000, and 4000 nM) were used to flow through the chip at a rate of 2 μL/s with an association time of 300 s and a dissociation time of 300 s. After each measurement cycle, the chip surface was regenerated with a solution of glycine-HCl (pH 2.0) followed by a PBS running buffer washing to remove bound proteins which enables the sensor chip to be reused for additional analyte injections. Real-time binding signals were recorded and analyzed by Data Analysis Module (Plexera Bioscience, Seattle, WA, USA). All possible binding curves were fitted by Langmuir equation, and the constants characterizing the association rate (or the on-rate, k_a or k_{on}), the dissociation rate (or the off-rate, k_d or k_{off}), and the equilibrium binding (K_D) were generated. In the SPR measurements, parallelly spotted mouse IgG (mIgG; Plexera Bioscience, Seattle, WA, USA) and bovine serum albumin (BSA; Plexera Bioscience, Seattle, WA, USA) on the chip with anti-mIgG (Plexera Bioscience,

Seattle, WA, USA) flowing past were used as positive and negative controls, respectively.

Catalytic activity assay for FdrA or FprA in the presence of Rv1786

The FdrA- or FprA-mediated reduction of cytochrome c in the presence of Rv1786 was measured in 50 mM potassium phosphate buffer (pH 7.5). The reaction mixture contained cytochrome c (Sangon Biotech, Shanghai, China), different molar ratio of FdrA:Rv1786 or FprA:Rv1786 (1:0, 1:1, 1:2, 1:4), and various concentrations of NAD(P)H (0–150 μM). The catalytic activity of Rv1786-dependent electron transferring towards cytochrome c was detected in a 96-well plate and monitored by PerkinElmer EnSpire® 2300 Multimode Plate Reader at 550 nm as described previously (Fischer et al. 2002; Zanno et al. 2005). All reactions were initiated by adding the substrate, NAD(P)H, and recorded in triplicate over a period of 1 min. Steady-state kinetic parameters for each cytochrome c assay were determined with a constant concentration of cytochrome c (500 μM) and varying the concentrations of NADH or NADPH. Unless otherwise stated, NADH and NADPH were substrates for FdrA-Rv1786 and FprA-Rv1786 reaction systems, respectively (Fischer et al. 2002; Zanno et al. 2005). All data manipulation and analysis were performed using SigmaPlot 13.0.

Results

Sequence similarity analysis of [3Fe-4S] ferredoxins across *Mycobacterium* genus

As indicated in Fig. 1a, b, the sequence similarity and a phylogenetic tree of the amino acid sequences of Rv1786 were analyzed in different mycobacterial species. The highlighted regions in Fig. 1 display a CXXHXXC(X)nCP motif, which is a typical iron-sulfur cluster-binding domain found in [3Fe-4S] cluster-containing ferredoxins. An alignment of the Rv1786 orthologs revealed that Rv1786 is highly conserved in different *Mtb* strains (100% identity) and among closely related *M. tuberculosis* complex (MTBC) species, which includes *Mycobacterium canettii* (99%), *Mycobacterium africanum* (99%), and *Mycobacterium bovis* (96%). Although sequence identities of Rv1786 orthologs remain considerable high in other pathogenic mycobacterial species such as *Mycobacterium kansasii* (86%) and *Mycobacterium marinum* (80%), lower similarities were obtained in a non-pathogenic mycobacterial member, *Mycobacterium smegmatis* (37%). When aligning with Rv1786 orthologs from bacteria outside the genus *Mycobacterium* including *Rhodopseudomonas palustris* (36%), *Bacillus thermoproteolyticus* (31%), and *Terrabacter species* (23%), sequence identities matched low (Shirakawa et al. 2005; Takagi et al. 2005; Zhang et al. 2014). In addition, Rv1786 shares low similarities with FdxD (32%) and FdX (31%), the other two [3Fe-4S] cluster-containing ferredoxins expressed in *Mtb* H37Rv (Fig. 1a, b). Rv1786 also shows low sequence similarity with Fdmor, a [3Fe-4S] cluster-containing ferredoxin encoded by part of morABC operon region from *Mycobacterium* sp. strain HE5 (29%) and an intracellular redox sensor WhiB3 (31%) from *Mtb* H37Rv (Sielaff et al. 2001; Singh et al. 2007).

Heterologous expression and spectroscopic properties of Rv1786, FdrA, FprA, and CYP143A1

Mtb Rv1786, FdrA, FprA, and CYP143A1 were expressed in the T7-based vector pET30a with C-terminal His-tag in *E. coli* as described in the "Materials and methods" section. All the His-tagged proteins could be obtained in soluble forms from *E. coli* lysates, and all the affinity-purified fractions from the nickel-charged resin displayed a brown color, which indicates the presence of iron-sulfur clusters, even after the dialysis and purification procedures. The SDS-PAGE analysis of the purified *Mtb* proteins is shown in Fig. 2a–d. FdrA, FprA, and CYP143A1 were all electrophoretically pure and shown to have approximate apparent masses of 48, 53, and 45.9 kDa, respectively, consistent with the expected masses from the amino acid sequences of the respective forms of the His-tagged proteins as previously reported (Fischer et al. 2002; Swami 2015; Zanno et al. 2005). However, the SDS-PAGE of Rv1786 provided an estimated molecular mass of about 17 kDa (Fig. 2d), that is about 9 kDa larger than its predicted molecular weight (7.93 kDa). To validate that the protein band corresponded to the expected Rv1786-His protein, we verified by western blot analysis that the His-tagged fusion protein could be detected using anti-His antibodies (Fig. 2e). To further confirm the identity of the protein, we used MALDI-TOF/TOF-MS where a major peak was obtained at 7935.8 Da, which is consistent with the theoretical average molecular mass of 7933.8 Da (Fig. 3). In order to confirm the iron-sulfur clusters ligated in the *Mtb* proteins, UV/Vis absorption spectra were collected using the scanning mode of PerkinElmer EnSpire® 2300 Multimode Plate Reader. As shown in Fig. 4a, a typical ferredoxin spectrum was obtained with a pliable peak at 406 nm for Rv1786. The outline of the UV/Vis absorption spectrum of Rv1786 is similar to FdX's except for missing a shoulder of ~450 nm (Imai et al. 1983; Ricagno et al. 2007; McLean et al. 2006c). The UV/Vis spectrum of CYP143A1 is shown in Fig. 4b. Pure ferric CYP143A1 has a typical P450 UV/Visible spectrum, with a Soret band at 416 nm, and Q-bands at ~572 and 535 nm, which is consistent with results reported previously (Swami 2015). The UV/Vis spectra of FdrA and FprA (Fig. 4c, d) are exactly the same as was reported previously (Fig. 4c, d) (Fischer et al. 2002; Zanno et al. 2005).

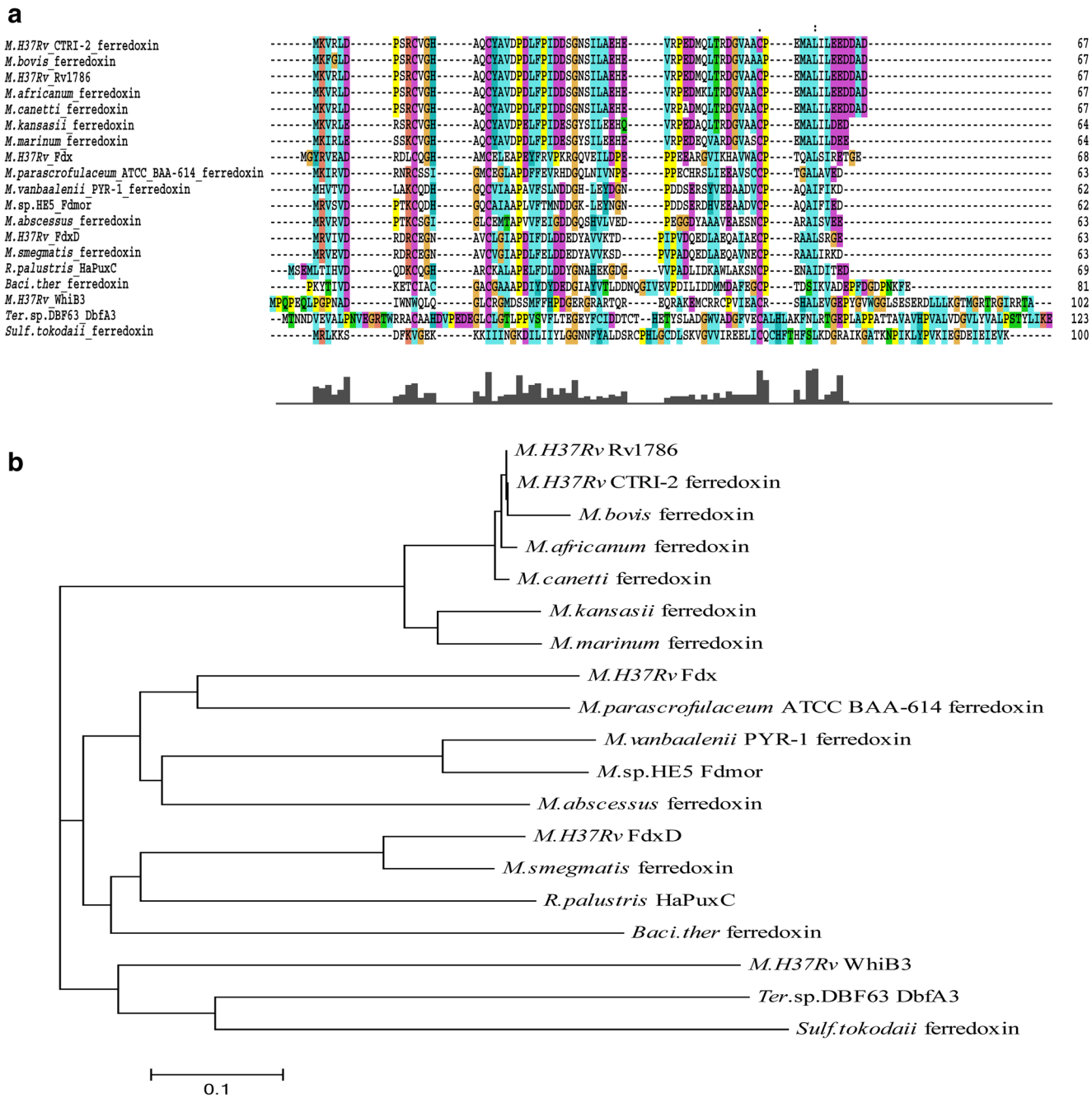

Fig. 1 Sequence alignment and phylogenetic analysis for Rv1786. **a** Alignment of the amino acid sequences of [3Fe-4S] ferredoxins in different species. **b** Phylogenetic tree illustrating the evolutionary relationship between Rv1786 and other [3Fe-4S] ferredoxins in different species. Bacterial species and the DDBJ/EMBL/GenBank reference sequences of the [3Fe-4S] ferredoxins included *M. tuberculosis* H37Rv (Rv1786 NP_216302, Fdx AFN48639, FdxD NP_218020, WhiB3 NP_217933), *M. tuberculosis* CTRI-2 (ferredoxin AEN00239), *M. bovis* (ferredoxin WP_019284145), *M. africanum* (ferredoxin WP_031669679), *M. canettii* (ferredoxin WP_014000948), *M. kansasii* (ferredoxin WP_023363981), *M. marinum* (ferredoxin WP_011740946), *M. parascrofulaceum* ATCC BAA-614 (ferredoxin EFG79933), *M. vanbaalenii* PYR-1 (ferredoxin AAS49916), *M.* sp. HE5 (Fdmor AAV54065), *M. abscessus* (ferredoxin CPY35196), *M. smegmatis* (ferredoxin WP_003897302), *R. palustris* Haa2 (HaPuxC 4ID8_A). *Baci. thermoproteolyticus* (ferredoxin 1WTF-A), *Ter.* sp. DBF63 (DbfA3 BAJ39939), *Sulf. tokodaii* str. 7 (ferredoxin BAB67388)

EPR spectroscopic analysis of Rv1786

EPR spectroscopy has long been the method of choice for revealing structural information of iron-sulfur cluster-containing proteins, such as ferredoxins. EPR X-band spectra were monitored for Rv1786 to provide further insights into the heme ligation environment and spin-state equilibrium in the external status. As shown in Fig. 5, the EPR signal for Rv1786 is

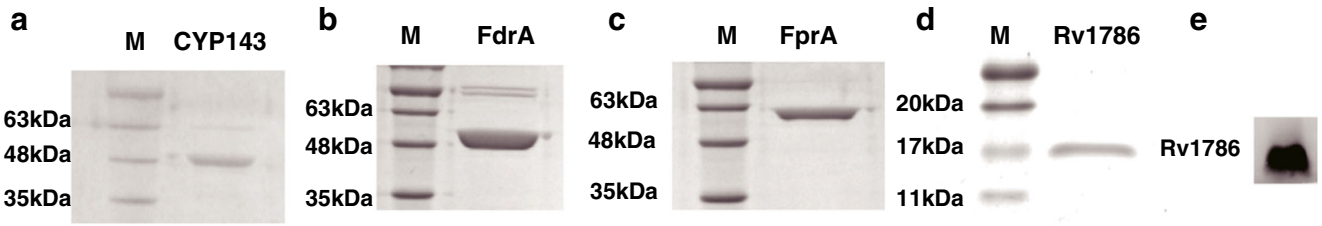

Fig. 2 SDS-PAGE of purified recombinant proteins. **a** CYP143A1. **b** FdrA. **c** FprA. **d** Rv1786. Proteins were stained with Coomassie blue in 12% gel. *Lane M* indicates size-marker proteins. **e** Expression of His-tagged Rv1786 detected by Western blot

typical for a [3Fe-4S] cluster-containing protein, with a strong $g = 2.02$ resonance, characteristic of $[3Fe\text{-}4S]^{+}S = 1/2$ clusters, which is in agreement with the EPR result of FdX, the only *Mtb* [3Fe-4S] ferredoxin member being well characterized in detail to date (Cheng et al. 2013; Kyritsis et al. 1999; Liu et al. 2013; McLean et al. 2006c).

Detection of interactions between Rv1786 and putative redox partners by SPR

SPR is an optical technique for detection of interactions between two different molecules, in which one is mobile and one is fixed on a thin gold film (Drescher et al. 2009). To discover the interaction modes between Rv1786 and putative redox partners including ferredoxin-NAD(P)H reductase FprA, FdrA, and CYP143A1, SPR analyses were used to explore the affinity between the proteins (Fig. 6 and Fig. S1). As shown in Fig. 6 and Fig. S1b–d, the interaction bindings of FprA, FdrA, and CYP143A1 with Rv1786 revealed that each of the three proteins displayed binding capacity to Rv1786, yet at different levels, and with signal intensities increasing with increasing concentration of the proteins. The SPR response signals of the controls are presented in Fig. S1a. The binding signal of the negative control (BSA) appeared flatlined as the baseline due to a very low non-specific binding. The FdrA and FprA showed a significant binding affinity to Rv1786 with K_D values of 2.59×10^{-6} and 1.14×10^{-6} M, respectively, while CYP143A1 showed an affinity to Rv1786 with a K_D value of 3.37×10^{-7} M, which is about 10 times lower than that of the two FNRs (Table 2). Since the lower the value of K_D corresponds to the more tight binding between proteins, it was indicated that CYP143A1 has a significantly

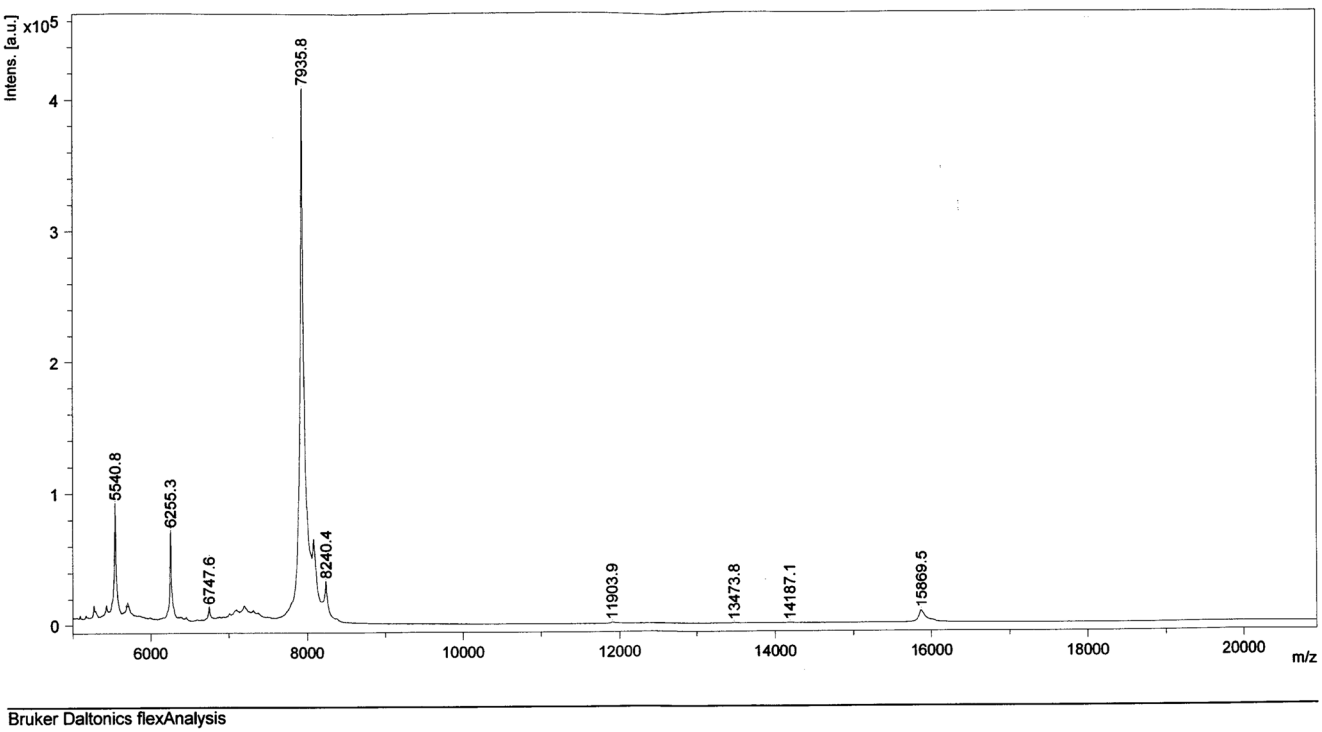

Fig. 3 Identification of Rv1786 molecular weight by MALDI-TOF/TOF MS analysis. The main ion peak obtained was 7935.8 Da, which was consistent with the theoretical average molecular mass 7933.81 Da

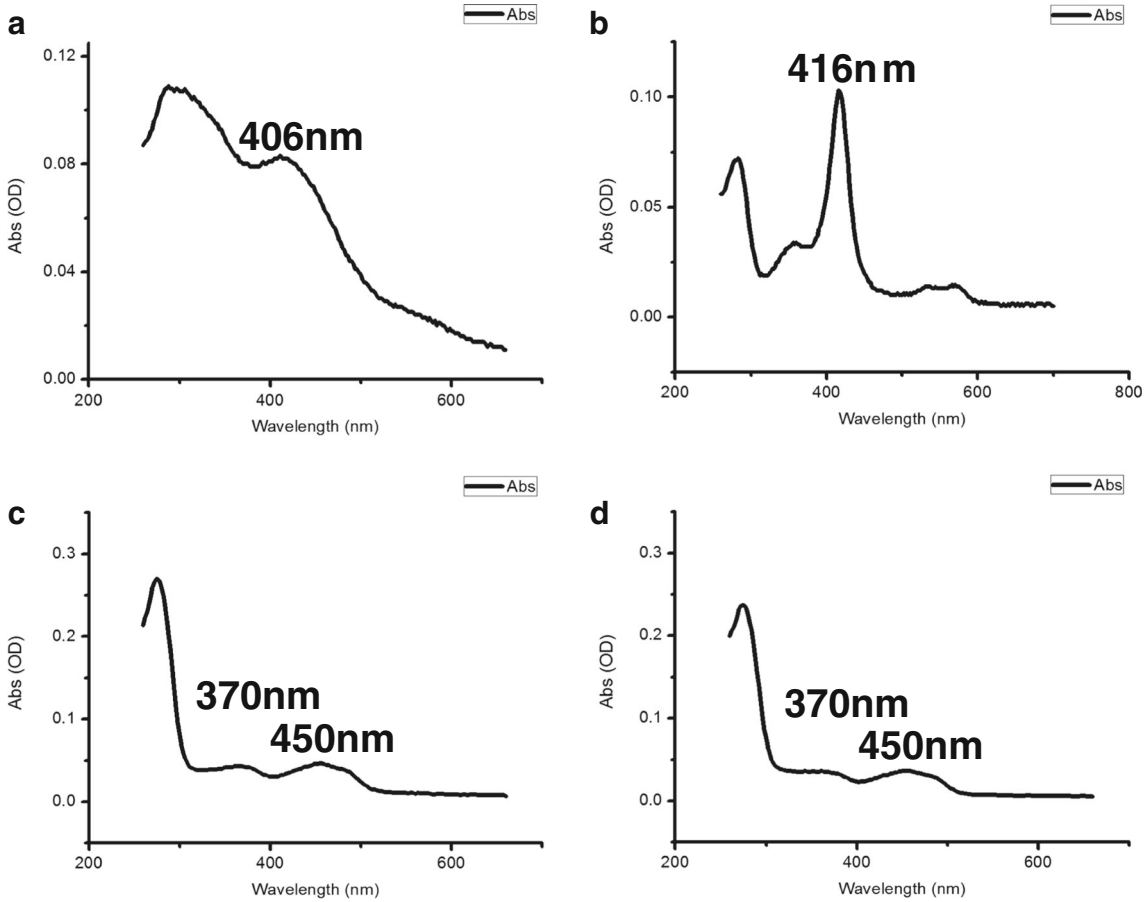

Fig. 4 UV/Vis absorption spectra of purified recombinant proteins. **a** Rv1786. **b** CYP143A1. **c** FdrA. **d** FprA. Samples were dissolved in potassium phosphate buffer (pH 7.4). The spectra were recorded at room temperature between 260 and 660 nm. The Soret spectral maxima are at 406, 416, 370, and 450 nm, respectively

higher affinity for Rv1786 than FdrA or FprA. Based on the ratio of the experimentally off- and on-rate (k_d/k_a) as well as rank order distributions of the equilibrium binding constants (K_D, equals to k_d/k_a) for each Rv1786-based coupling on an on-off quadrant plot as shown in Table 2 and Fig. 6, affinity reactions between Rv1786 and each of FdrA, FprA, and CYP143A1 can be described as a slower on-rate/faster off-rate binding, a faster on-rate/faster off-rate binding, and a faster on-rate/slower off-rate binding (Fig. 6), respectively.

Steady state kinetic assay

Since NADH and NADPH were characterized as efficient reductants for FdrA and FprA, respectively, the capacity of Rv1786-mediated electron transferring towards the final electron acceptor, cytochrome c, was determined in the presence of NADH-FdrA or NADPH-FprA in steady-state kinetic assays (Fischer et al. 2002; Zanno et al. 2005). The kinetic constants for two FNRs (FdrA or FprA) coupled with increasing quantities of Rv1786 in the presence of the substrate are listed in Tables 3 and 4. A weak cytochrome c reductase activity was monitored for both FdrA and FprA in the absence of the ferredoxin Rv1786 as electron transfer protein (FdrA $k_{cat} = 2.396 \pm 0.160\ min^{-1}$, $K_m = 2.762 \pm 0.758\ \mu M$, $k_{cat}/K_m = 0.87 \times 10^6\ M^{-1}\ min^{-1}$; FprA $k_{cat} = 2.988 \pm 0.476\ min^{-1}$, $K_m = 10.65 \pm 2.75\ \mu M$, $k_{cat}/K_m = 0.28 \times 10^6\ M^{-1}\ min^{-1}$). In comparison with FdrA alone, the reduction rate and efficiency of cytochrome c showed approximately a 22- to 45-fold higher ($k_{cat} = 68.16 \pm 4.16$ to $111.2 \pm 1.8\ min^{-1}$, $k_{cat}/K_m = 1.91 \times 10^7$ to $3.91 \times 10^7\ M^{-1}\ min^{-1}$) for FdrA in the presence of varying levels of Rv1786. The overall catalytic efficiency of the reaction is also faster for FprA with supplement of Rv1786 ($k_{cat} = 4.909 \pm 0.273$ to $7.785 \pm 1.210\ min^{-1}$ and $k_{cat}/K_m = 0.33 \times 10^6$ to $0.73 \times 10^6\ M^{-1}\ min^{-1}$ for FprA:Rv1786 compared with $k_{cat} = 2.988 \pm 0.476\ min^{-1}$, $k_{cat}/K_m = 0.28 \times 10^6\ M^{-1}\ min^{-1}$ for FprA alone), though the parameters were not altered as significantly as what observed in NAPDH-FdrA-Rv1786-cytochrome c catalytic system. However, the K_m values for FdrA or FprA remain relatively constant in the absence or presence of varying levels of Rv1786, which suggests that Rv1786 has little effect on the affinity of the two FNRs for the cytochrome c.

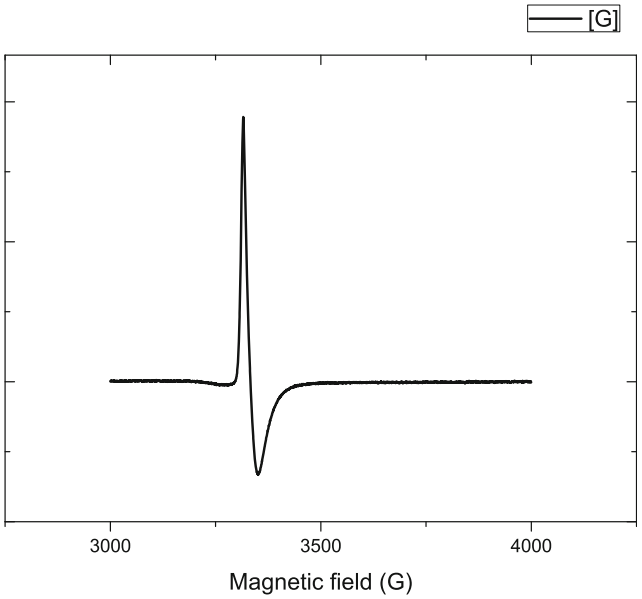

Fig. 5 EPR spectra of Rv1786. EPR spectra of oxidized Mtb Rv1786 were recorded at a concentration of 1.25 mg/mL in 50 mM Tris buffer at 10 K. Instrument settings were as follows: microwave frequency = 9.371 GHz, microwave power = 2.377 mW, sweep time = 120 s, modulation amplitude = 1.000 G. No EPR signal was detectable for the dithionite-reduced Rv1786

Discussion

Revealing the biochemical features of uncharacterized proteins in *Mtb* will extend our understanding of key life processes required for the pathogen in infection, latency, and proliferation, which will help us to identify essential structural or functional proteins as potential target for the development of new drugs against the pathogen. The *Mtb* genome encodes a limited number of ferredoxins, FNRs or fusions of ferredoxin, and FNR-like domains that function as putative electron transfers to support the catalytic activities of up to 20 different CYP enzymes (Munro et al. 2003; Ouellet et al. 2010). The *Mtb* CYPs are putative drug target proteins due to their essential roles in the complex lipid metabolism of *Mtb* and their high-affinity binding to anti-fungal azole drugs (Zhang et al. 2006). The number of ferredoxin and FNR genes is thus significantly fewer than the CYP genes in the *Mtb* genome. Thus, the CYP enzymes and their putative redox partners cannot have a one-to-one relationship, which suggests that these redox proteins could play a "hub-like" role in the CYP-associated electron transfer pathways. Despite the importance of the redox proteins in CYP-related catalytic processes in *Mtb*, the structural or functional properties for the majority of the putative *Mtb* ferredoxins remain unclear. Among the uncharacterized *Mtb* ferredoxins, Rv1786 is one of the most obvious candidates for CYP-related redox partners, as it is adjacent to the CYP143A1 (*Rv1785c*) in the chromosome. Considering that correct ferredoxin-FNR coupling is a prerequisite for efficiency of electron transferring in the redox system, it is crucial to identify the effective combination of Rv1786 and putative endogenous FNRs or fusions containing FNR-like domains from *Mtb* (Lewis and Hlavica 2000).

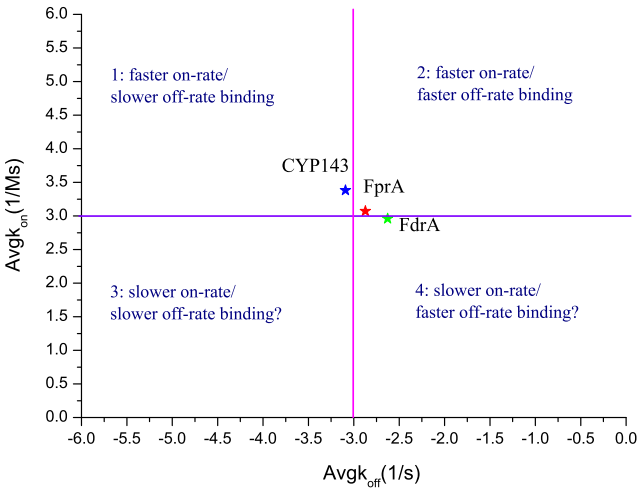

Fig. 6 Distribution of kinetic parameters of protein-protein interactions determined by SPR on an on-off quadrant plot. Rv1786 was dissolved in 25 mM Tris-HCl (pH 8.0) and immobilized onto a Nanocapture sensor chip (Plexera Bioscience, Seattle, WA, USA) by QArray mini spotter (Genetix Ltd., New Milton, Hampshire, UK). The purified FdrA, FprA, or CYP143A1 was then injected as analyte at various concentrations in the running buffer for detecting their binding affinity to Rv1786 spotted on the chip surface. Four different concentrations of each analyte protein (500, 1000, 2000, and 4000 nM) were used to flow through the chip. All possible binding curves were fitted by Langmuir equation, and the constants characterizing the on-rate (k_{on}), the off-rate (k_{off}), and the equilibrium binding (K_D) were generated

In the present study, we identified by phylogenetic analysis that Rv1786 has a typical CXXHXXC(X)nCP iron-sulfur cluster-binding motif and is highly conserved among pathogenic members of *Mycobacterium* genus. These data suggests that the ferredoxin may be relevant for full virulence or infectivity of *Mtb* towards the human host. The genome sequence of *Mtb* H37Rv revealed two FNRs, FdrA (*Rv0688*) and FprA (*Rv0886*), as putative electron transfer partner proteins for ferredoxins (Ouellet et al. 2010). Since we can express both *Mtb* FNR proteins in a soluble and a stable form in *E. coli*, it is possible to reconstitute potential combinations between Rv1786 and each of the two FNRs in vitro (Fischer et al. 2002; Zanno et al. 2005). Based on the mobility in SDS-PAGE of the purified recombinant *Mtb* Rv1786, the molecular weight of the protein was estimated to be 17 kDa, which is obviously bigger than the prediction by the sequence of the His-tagged Rv1786. However, our MS analysis confirmed that the mass of the protein correlated to the predicted molecular mass, a result which also indicated that the reason to the protein retardation of the SDS-PAGE could not be due to a post-translational modification. However, the unpredicted migration behavior of the protein could instead be related to its acidic nature. It has been observed in other studies that acidic proteins (i.e., glutamate- and/or aspartate-rich proteins) often display a larger molecular mass in SDS-PAGE analysis than

Table 2 Binding parameters of SPR measurements

Mobile protein	Fixed protein	k_a (10^3 M^{-1} s^{-1})	k_d (10^{-3} s^{-1})	K_D (10^{-6} M)
FdrA	Rv1786	0.912	2.36	2.59
FprA	Rv1786	1.18	1.34	1.14
CYP143A1	Rv1786	2.41	0.811	0.337

Table 3 Kinetic parameters for reductase activity of FdrA coupled by series concentration of Rv1786

Donor	FdrA:Rv1786	k_{cat} (min^{-1})	K_m (μM)	k_{cat}/K_m (M^{-1} min^{-1})	$(k_{cat}/K_m)^{FdrA:Rv1786}/(k_{cat}/K_m)^{FdrA}$
NADH	1:0	2.396 ± 0.160	2.762 ± 0.758	0.87×10^6	1.00
NADH	1:1	68.16 ± 4.16	3.567 ± 0.721	1.91×10^7	22.0
NADH	1:2	94.20 ± 2.81	3.668 ± 0.578	2.57×10^7	29.5
NADH	1:4	111.2 ± 1.8	2.843 ± 0.135	3.91×10^7	45.0

their predicted size (Guan et al. 2014; Niu and Guiltinan 1994; Sallantin et al. 1990). Considering that Rv1786 is a typical acidic protein with a high percentage (23.9%) of glutamate and aspartate residues and with a pI of 4.11, this could also be the explanation behind our SDS-PAGE result. The UV/Vis and EPR spectroscopic properties of the purified Rv1786 confirmed that the ferredoxin contained a [3Fe-4S] cluster and was folded correctly as proposed upon recombinant expression in *E. coli*.

The different affinity interactions between Rv1786 and each of FdrA, FprA, and CYP143A1 were analyzed with SPR measurements. According to the commonly accepted quantification standard of interaction features in SPR analyses, a significant protein-protein binding affinity can be demonstrated with the equilibrium binding constants (K_D) at 10^{-6} M level and an experimentally off- and on-rate can be ranked with 10^{-3} s^{-1} and 10^3 M^{-1} s^{-1} level as fast/slow cutoffs (Hu et al. 2014; Wu et al. 2015; Zhu et al. 2014). In the present study, a significant affinity coupling of Rv1786 to each of FdrA and FprA has been identified with K_D values at 10^{-6} level. When comparing k_d and k_a values between Rv1786-FdrA and Rv1786-FprA couplings, a slightly stronger binding (a faster on-rate and a slower off-rate) is observed for Rv1786-FprA. In agreement with the prediction in terms of their genetic context, a significant binding affinity between Rv1786 and CYP143A1 was also demonstrated with k_d, k_a, and K_D values at 10^{-4} s^{-1}, 10^3 M^{-1} s^{-1}, and 10^{-7} M level.

Since *Rv1786* lies adjacent to the gene encoding CYP143A1 (*Rv1785c*), the protein encoded by the gene has been thought as a natural electron transferring partner for CYP143A1 in Mtb (McLean and Munro 2008; Ouellet et al. 2010). However, as the substrate for the CYP143A1 enzyme still remains unknown, the electron transfer function of Rv1786 is difficult to evaluate in an authentic CYP143A1-based catalytic reaction system. Considering that cytochrome c has been used for evaluation of the electron transfer activity of *Mtb* FdrA or FprA coupling with other *Mtb* ferredoxins in previous studies (Fischer et al. 2002; Zanno et al. 2005), we decided to use the enzyme as final electron acceptor to characterize the preference for the two FNRs in the absence or presence of Rv1786. The cytochrome c reduction assay demonstrates that Rv1786 can significantly enhance the catalytic rate and efficiency of the reduction reaction for both FdrA and FprA. The steady-state kinetic parameters for FdrA-Rv1786 suggest a better coupling activity of Rv1786 to FdrA than that of Rv1786 to FprA.

In summary, the observations from the present study provide a preliminary but rational evidence for characterization of Rv1786 as an active electron transfer in CYP-associated redox system in *Mtb*. Our results indicate that Rv1786 is able to couple with FdrA or FprA as redox partner. A better coupling activity was observed with FdrA while a stronger binding was found with FprA. Further studies involving Rv1786-deficient systems, crystal structure characterization, and exact function

Table 4 Kinetic parameters for reductase activity of FprA coupled by series concentration of Rv1786

Donor	FprA:Rv1786	k_{cat} (min^{-1})	K_m (μM)	k_{cat}/K_m (M^{-1} min^{-1})	$(k_{cat}/K_m)^{FprA:Rv1786}/(k_{cat}/K_m)^{FprA}$
NADPH	1:0	2.988 ± 0.476	10.65 ± 2.75	0.28×10^6	1.00
NADPH	1:1	4.909 ± 0.273	14.94 ± 4.81	0.33×10^6	1.17
NADPH	1:2	6.841 ± 0.847	12.36 ± 2.35	0.55×10^6	1.98
NADPH	1:4	7.785 ± 1.210	10.57 ± 2.66	0.73×10^6	2.63

in CYP143A1, catalytic reactions would be required to fully estimate the extent of involvement of this important ferredoxin in virulence or infectivity of *Mtb*. The present study improves our understanding of the biochemical properties and function of the iron-sulfur cluster containing ferredoxin proteins in *Mtb*.

Acknowledgments The authors acknowledge Birgitta Henriques-Normark, Mikael Rhen, Peter Mellroth, and Lu-Ni Chen (Karolinska Institutet) for the critical review, data discussion, and text modification of this manuscript, as well as Yu Lu and Jian Xu for providing the genomic DNA from *Mtb* H37Rv used in this study.

Author contributions XYY and XFY conceived and coordinated the study. YL and XYY designed the major experiments. XFY, CRL, and JDJ provided suggestions on the research plan and contributed ideas to the research proposal. YL carried out the major study work. FQ performed the experiments shown in Tables 3 and 4. YL (Yue Li) contributed to preparation of purified FdrA and FprA. XHS performed the western blot as shown in Fig. 2e. YL, XYY, and XFY analyzed and discussed the data. YL, XYY, and XFY wrote and refined the manuscript. All authors reviewed the results and approved the final version of the manuscript.

Compliance with ethical standards

Funding This research was supported by the National Natural Science Foundation of China (NSFC) (81273427 to XYY, 81361138020 to JDJ, and 81573475 to CRL), the National Mega-project for Innovative Drugs (2014ZX09507-009 to XFY), the Beijing Science and Technology Projects (Z141102004414065 and Z151100000315029 to XFY), CAMS Initiative Fund for Innovative Medicine (2016-I2M-3-014 to XFY), and the Peking Union Medical College (PUMC) Youth Fund (33320140177 and 3332016139 to XYY). XYY and CRL were supported by the China Scholarship Council (CSC) State-Sponsored Scholarship Program for Visiting Scholars in Sweden/Europe (CSC2014-3012/201408110091-2).

Conflict of interest The authors declare that they have no conflict of interest.

Ethical approval This article does not contain any studies with human participants or animals performed by any of the authors.

References

Cheng VW, Tran QM, Boroumand N, Rothery RA, Maklashina E, Cecchini G, Weiner JH (2013) A conserved lysine residue controls iron-sulfur cluster redox chemistry in *Escherichia coli* fumarate reductase. Biochim Biophys Acta 1827(10):1141–1147. doi:10.1016/j.bbabio.2013.05.004

Drescher DG, Ramakrishnan NA, Drescher MJ (2009) Surface plasmon resonance (SPR) analysis of binding interactions of proteins in inner-ear sensory epithelia. Methods Mol Biol 493:323–343. doi:10.1007/978-1-59745-523-7_20

Ewen KM, Hannemann F, Iametti S, Morleo A, Bernhardt R (2011) Functional characterization of Fdx1: evidence for an evolutionary relationship between P450-type and ISC-type ferredoxins. J Mol Biol 413(5):940–951. doi:10.1016/j.jmb.2011.09.010

Fischer F, Raimondi D, Aliverti A, Zanetti G (2002) *Mycobacterium tuberculosis* FprA, a novel bacterial NADPH-ferredoxin reductase. Eur J Biochem 269(12):3005–3013. doi:10.1046/j.1432-1033.2002.02989.x

Guan Y, Zhu Q, Huang D, Zhao S, Li JL, Peng J (2014) An equation to estimate the difference between theoretically predicted and SDS PAGE-displayed molecular weights for an acidic peptide. Sci Rep 5:13370. doi:10.1038/srep13370

Hu Z, Lausted C, Yoo H, Yan X, Brightman A, Chen J, Wang W, Bu X, Hood L (2014) Quantitative liver-specific protein fingerprint in blood: a signature for hepatotoxicity. Theranostics 4(2):215–228. doi:10.7150/thno.7868

Imai T, Matsumoto T, Ohta S, Ohmori D, Suzuki K, Tanaka J, Tsukioka M, Tobari J (1983) Isolation and characterization of a ferredoxin from *Mycobacterium smegmatis* Takeo. Biochim Biophys Acta 743(1):91–97. doi:10.1016/0167-4838(83)90421-1

Kyritsis P, Kummerle R, Huber JG, Gaillard J, Guigliarelli B, Popescu C, Munck E, Moulis JM (1999) Unusual NMR, EPR, and Mossbauer properties of *Chromatium vinosum* 2[4Fe-4S] ferredoxin. Biochemistry 38(19):6335–6345. doi:10.1021/bi982894u

Lauzardo M, Peloquin CA (2012) Antituberculosis therapy for 2012 and beyond. Expert Opin Pharmacother 13(4):511–526. doi:10.1517/14656566.2012.657176

Lewis DF, Hlavica P (2000) Interactions between redox partners in various cytochrome P450 systems: functional and structural aspects. Biochim Biophys Acta 1460(2–3):353–374. doi:10.1016/S0005-2728(00)00202-4

Liu Y, Guo S, Yu R, Ji J, Qiu G (2013) HdrC2 from *Acidithiobacillus* ferrooxidans owns two iron-sulfur binding motifs but binds only one variable cluster between [4Fe-4S] and [3Fe-4S]. Curr Microbiol 66(1):88–95. doi:10.1007/s00284-012-0244-y

McLean KJ, Munro AW (2008) Structural biology and biochemistry of cytochrome P450 systems in *Mycobacterium tuberculosis*. Drug Metab Rev 40(3):427–446. doi:10.1080/03602530802186389

McLean KJ, Clift D, Lewis DG, Sabri M, Balding PR, Sutcliffe MJ, Leys D, Munro AW (2006a) The preponderance of P450s in the *Mycobacterium tuberculosis* genome. Trends Microbiol 14(5):220–228. doi:10.1016/j.tim.2006.03.002

McLean KJ, Dunford AJ, Sabri M, Neeli R, Girvan HM, Balding PR, Leys D, Seward HE, Marshall KR, Munro AW (2006b) CYP121, CYP51 and associated redox systems in *Mycobacterium tuberculosis*: towards deconvoluting enzymology of P450 systems in a human pathogen. Biochem Soc Trans 34(Pt 6):1178–1182. doi:10.1042/BST0341178

McLean KJ, Warman AJ, Seward HE, Marshall KR, Girvan HM, Cheesman MR, Waterman MR, Munro AW (2006c) Biophysical characterization of the sterol demethylase P450 from *Mycobacterium tuberculosis*, its cognate ferredoxin, and their interactions. Biochemistry 45(27):8427–8443. doi:10.1021/bi0601609

Munro AW, McLean KJ, Marshall KR, Warman AJ, Lewis G, Roitel O, Sutcliffe MJ, Kemp CA, Modi S, Scrutton NS, Leys D (2003) Cytochromes P450: novel drug targets in the war against multidrug-resistant *Mycobacterium tuberculosis*. Biochem Soc Trans 31(Pt 3):625–630. doi:10.1042/bst0310625

Niu X, Guiltinan MJ (1994) DNA binding specificity of the wheat bZIP protein EmBP-1. Nucleic Acids Res 22(23):4969–4978

Oluwatoyin Japhet M, Adeyemi Adesina O, Famurewa O, Svensson L, Nordgren J (2012) Molecular epidemiology of rotavirus and norovirus in Ile-Ife, Nigeria: high prevalence of G12P[8] rotavirus strains and detection of a rare norovirus genotype. J Med Virol 84(9):1489–1496. doi:10.1002/jmv.23343

Ouellet H, Johnston JB, Ortiz de Montellano PR (2010) The *Mycobacterium tuberculosis* cytochrome P450 system. Arch Biochem Biophys 493(1):82–95. doi:10.1016/j.abb.2009.07.011

Ricagno S, de Rosa M, Aliverti A, Zanetti G, Bolognesi M (2007) The crystal structure of FdxA, a 7Fe ferredoxin from *Mycobacterium smegmatis*. Biochem Biophys Res Commun 360(1):97–102. doi:10.1016/j.bbrc.2007.06.013

Riccardi G, Pasca MR, Buroni S (2009) *Mycobacterium tuberculosis*: drug resistance and future perspectives. Future Microbiol 4(5): 597–614. doi:10.2217/fmb.09.20

Sallantin M, Huet JC, Demarteau C, Pernollet JC (1990) Reassessment of commercially available molecular weight standards for peptide sodium dodecyl sulfate polyacrylamide gel electrophoresis using electroblotting and microsequencing. Electrophoresis 11(1):34–36. doi:10.1002/elps.1150110108

Sambrook J, Russell DW (2006) The condensed protocols from molecular cloning: a laboratory manual. Cold Spring Harbor Laboratory Press, Cold Spring Harbor

Shirakawa T, Takahashi Y, Wada K, Hirota J, Takao T, Ohmori D, Fukuyama K (2005) Identification of variant molecules of *Bacillus thermoproteolyticus* ferredoxin: crystal structure reveals bound coenzyme A and an unexpected [3Fe-4S] cluster associated with a canonical [4Fe-4S] ligand motif. Biochemistry 44(37):12402–12410. doi:10.1021/bi0508441

Sielaff B, Andreesen JR, Schrader T (2001) A cytochrome P450 and a ferredoxin isolated from *Mycobacterium* sp. strain HE5 after growth on morpholine. Appl Microbiol Biotechnol 56(3–4):458–464. doi:10.1007/s002530100634

Singh A, Guidry L, Narasimhulu KV, Mai D, Trombley J, Redding KE, Giles GI, Lancaster JR Jr, Steyn AJ (2007) *Mycobacterium tuberculosis* WhiB3 responds to O_2 and nitric oxide via its [4Fe-4S] cluster and is essential for nutrient starvation survival. Proc Natl Acad Sci U S A 104(28):11562–11567. doi:10.1073/pnas.0700490104

Swami S (2015) Structure and biochemistry of the orphan cytochrome P450s CYP126A1 and CYP143A1 from the human pathogen *Mycobacterium tuberculosis*. Dissertation, University of Manchester Manchester Uk

Takagi T, Habe H, Yoshida T, Yamane H, Omori T, Nojiri H (2005) Characterization of [3Fe-4S] ferredoxin DbfA3, which functions in the angular dioxygenase system of *Terrabacter* sp. strain DBF63. Appl Microbiol Biotechnol 68(3):336–345. doi:10.1007/s00253-005-1928-z

Werck-Reichhart D, Feyereisen R (2000) Cytochromes P450: a success story. Genome Biol 1(6):reviews3003.1–reviews3003.9. doi:10.1186/gb-2000-1-6-reviews3003

World Health Organization (2016) Global tuberculosis report 2016. WHO website. http://www.who.int/tb/publications/global_report/en. Accessed 13 Oct 2016

Wu W, Li R, Li X, He J, Jiang S, Liu S, Yang J (2015) Quercetin as an antiviral agent inhibits influenza A virus (IAV) entry. Viruses 8(1):6. doi:10.3390/v8010006

Zanno A, Kwiatkowski N, Vaz AD, Guardiola-Diaz HM (2005) MT FdR: a ferredoxin reductase from *M. tuberculosis* that couples to MT CYP51. Biochim Biophys Acta 1707(2–3):157–169. doi:10.1016/j.bbabio.2004.11.010

Zhang Y, Post-Martens K, Denkin S (2006) New drug candidates and therapeutic targets for tuberculosis therapy. Drug Discov Today 11(1–2):21–27. doi:10.1016/S1359-6446(05)03626-3

Zhang T, Zhang A, Bell SG, Wong LL, Zhou W (2014) The structure of a novel electron-transfer ferredoxin from *Rhodopseudomonas palustris* HaA2 which contains a histidine residue in its iron-sulfur cluster-binding motif. Acta Crystallogr D Biol Crystallogr 70(Pt 5): 1453–1464. doi:10.1107/S139900471400474X

Zhu L, Wang K, Cui J, Liu H, Bu X, Ma H, Wang W, Gong H, Lausted C, Hood L, Yang G, Hu Z (2014) Label-free quantitative detection of tumor-derived exosomes through surface plasmon resonance imaging. Anal Chem 86(17):8857–8864. doi:10.1021/ac5023056